Adhesive and mechanical regulation of mesenchymal stem cell differentiation in human bone marrow and periosteum-derived progenitor cells

Jeroen Eyckmans[1,2,*], Grace L. Lin[1,*] and Christopher S. Chen[1,‡]

[1]Department of Bioengineering, University of Pennsylvania, 510 Skirkanich Hall, 210 South 33rd Street, Philadelphia, PA 19104, USA
[2]Laboratory for Skeletal Development and Joint Disorders, Katholieke Universiteit Leuven, Herestraat 49, Box 813, B-3000 Leuven, Belgium
*These authors contributed equally to this work
‡Author for correspondence (chrischen@seas.upenn.edu)

Biology Open 1, 1058–1068
doi: 10.1242/bio.20122162
Received 4th June 2012
Accepted 27th June 2012

Summary

It has previously been demonstrated that cell shape can influence commitment of human bone marrow-derived mesenchymal stem cells (hBMCs) to adipogenic, osteogenic, chondrogenic, and other lineages. Human periosteum-derived cells (hPDCs) exhibit multipotency similar to hBMCs, but hPDCs may offer enhanced potential for osteogenesis and chondrogenesis given their apparent endogenous role in bone and cartilage repair *in vivo*. Here, we examined whether hPDC differentiation is regulated by adhesive and mechanical cues comparable to that reported for hBMC differentiation. When cultured in the appropriate induction media, hPDCs at high cell seeding density demonstrated enhanced levels of adipogenic or chondrogenic markers as compared with hPDCs at low cell seeding density. Cell seeding density correlated inversely with projected area of cell spreading, and directly limiting cell spreading with micropatterned substrates promoted adipogenesis or chondrogenesis while substrates promoting cell spreading supported osteogenesis. Interestingly, cell seeding density influenced differentiation through both changes in cell shape and non-shape-mediated effects: density-dependent adipogenesis and chondrogenesis were regulated primarily by cell shape whereas non-shape effects strongly influenced osteogenic potential. Inhibition of cytoskeletal contractility by adding the Rho kinase inhibitor Y27632 further enhanced adipogenic differentiation and discouraged osteogenic differentiation of hPDCs. Together, our results suggest that multipotent lineage decisions of hPDCs are impacted by cell adhesive and mechanical cues, though to different extents than hBMCs. Thus, future studies of hPDCs and other primary stem cell populations with clinical potential should consider varying biophysical metrics for more thorough optimization of stem cell differentiation.

Key words: Mesenchymal stem cell differentiation, Mechanoregulation, Cell shape, Rho kinase, Adhesion

Introduction

Mesenchymal Stem/Stromal Cells (MSCs) are cell populations found in the stroma of mesenchymal tissues such as bone, bone marrow, cartilage, ligaments, and adipose tissue. Because these cell populations can be readily isolated from patients for expansion and differentiation *in vitro* into at least three different lineages (Augello and De Bari, 2010; Dominici et al., 2006; Pittenger et al., 1999), MSCs are of great interest for clinical therapies. Indeed, protocols for injections of autologous MSCs are already in clinical trials not only for various musculoskeletal tissue replacement therapies including bone, cartilage, and intervertebral discs, but also to treat organ failure (cardiac, lung, liver, pancreas among others) and autoimmune diseases (for reviews, see Gómez-Barrena et al., 2011; Trounson et al., 2011; Tyndall and Gratwohl, 2009). Moreover, MSCs are being developed as a critical cell source in tissue engineering, which involves the *ex vivo* creation of biological implants intended eventually to replace tissues or functional organs (Marcacci et al., 2007). However, the molecular mechanisms regulating MSC differentiation into the desired terminal lineages are still incompletely understood, impeding efforts to generate useful clinical products from primary cells obtained from patients.

To study MSC differentiation, an array of *in vitro* assays has been developed. To drive osteogenic differentiation, MSCs are cultured in a serum-containing medium supplemented with dexamethasone, ascorbic acid, and beta-glycerophosphate (Jaiswal et al., 1997; Pittenger et al., 1999). Adipogenesis is induced by insulin, isobutyl-methylxanthine, dexamethasone, and indomethacin (Sekiya et al., 2004), and chondrogenesis is induced in serum-free medium supplemented with TGFβ (Johnstone et al., 1998). Utilizing these media, the differentiation capacities of MSCs derived from different tissues and species have been compared. As virtually all of these can undergo *in vitro* multilineage differentiation, differences between MSCs have been reported mostly in terms of differentiation efficiency in response to differentiation cocktails for the different lineages (Boeuf and Richter, 2010;

Noël et al., 2008; Sakaguchi et al., 2005). However, these comparisons are predicated on the notion that the primary driving factor for MSC differentiation is soluble factors, which may not be true.

Biophysical cues from the microenvironment and neighboring cells may also contribute to the lineage fate and differentiation efficiency of MSCs. For example, seeding density has been shown to impact the efficiency of adipogenesis (Lu et al., 2009) or chondrogenesis *in vitro* (Nakahara et al., 1991a; Seghatoleslami and Tuan, 2002), and our group and others have demonstrated that lineage commitment of human bone marrow-derived cells (hBMCs) to osteogenesis/adipogenesis (Kilian et al., 2010; McBeath et al., 2004) or myofibroblastogenesis/chondrogenesis (Gao et al., 2010) is in part regulated by cell shape and/or RhoA-mediated cytoskeletal tension. Despite the central role of cell shape and cytoskeletal forces in regulating hBMCs, these findings have not been extended to MSCs from other tissue sources. Thus, the reported differences in differentiation efficiency between various MSC types may partially originate from differences in mechanotransduction in these other MSC types. It is even possible that poor differentiation of varying MSC types could be rescued by manipulating adhesive or mechanical parameters.

Similar to hBMCs, human periosteum-derived cells (hPDCs) display MSC-like multipotency from single cell-derived clonal populations (De Bari et al., 2006) and contribute to robust bone and cartilage growth and repair *in vivo* (Colnot, 2009; De Bari et al., 2006; Eyckmans and Luyten, 2006). hPDCs are distinct from hBMCs in their tissue of origin, but both cell types arise from mesoderm-derived populations during embryonic development. Because periosteal cells, not bone marrow cells, predominantly contribute to fracture healing in postnatal life (Colnot, 2009; Maes et al., 2010), hPDCs may even be a more suitable cell population for bone engineering applications (Agata et al., 2007; Zhu et al., 2006). Thus hPDCs are a clinically relevant source of primary mesenchymal progenitors that is currently understudied in regard to its molecular regulation of differentiation (Mahajan, 2012), particularly as hPDC-based bone grafts are already being used in the clinic to treat patients (Trautvetter et al., 2011).

Although *in vitro* differentiation assays for hPDCs were successfully adopted from media conditions used for hBMCs, in this paper, we report a comparison of the effects of biophysical conditions on differentiation of these two primary human MSCs. In particular, we examine the role of cell seeding density, cell shape, and RhoA-mediated cytoskeletal tension on mesenchymal stem cell differentiation *in vitro* to osteogenic, adipogenic, and chondrogenic lineages.

Results

Population dynamics of hBMCs and hPDCs in culture

Cell seeding density, or the number of cells plated per square cm, impacts cell behavior. Our previous studies showed a link between cell seeding density and proliferation rates in multiple cell types (Nelson and Chen, 2002), and between seeding density and differentiation efficiency in MSCs (McBeath et al., 2004). Thus, we first compared the proliferation rates of hBMCs and hPDCs under different seeding densities. Independently of the cell culture vessel used, hPDCs proliferated faster than hBMCs and reached full confluence after 10 days (Fig. 1A) when initially seeded at low seeding density (5000 cells/cm^2). In addition, the cell density of hPDCs obtained at confluence was consistently higher as compared to hBMCs, which suggested that hPDCs are smaller than hBMCs. Indeed, side-by-side comparison of adherent hBMC and hPDC populations under phase contrast microscopy suggested that hBMCs were more spread on tissue culture plastic with a broader cytoplasmic body than hPDCs (Fig. 1B, white arrows), whereas hPDCs displayed a more spindle-shaped phenotype (Fig. 1B, black arrows).

To examine how initial seeding density impacted hBMC and hPDC populations, we empirically chose three seeding densities, 5000 (5 k/cm^2), 25000 (25 k/cm^2), and 85000 (85 k/cm^2). When seeded at 5 k/cm^2, both hPDCs and hBMCs attached efficiently as mostly isolated cells with few if any cell–cell contacts. At

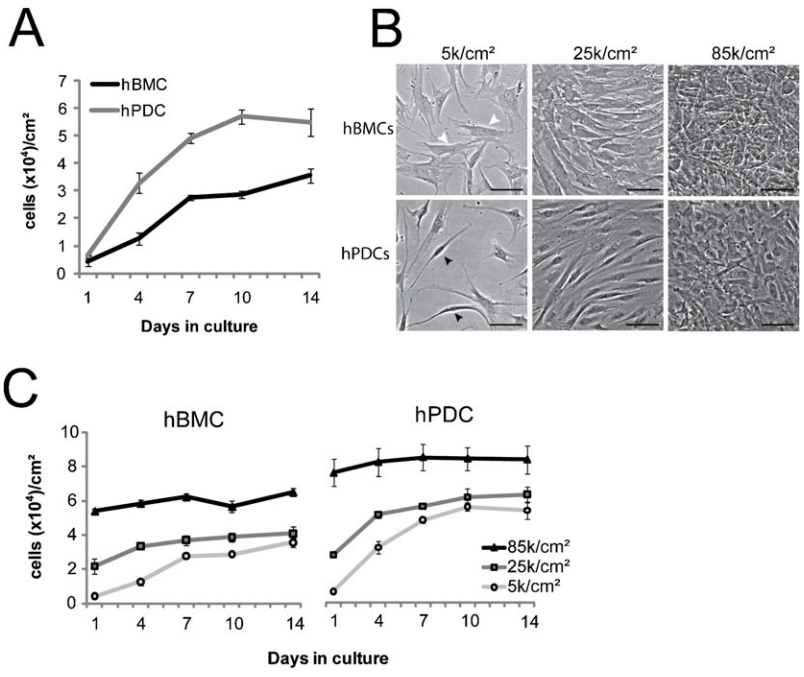

Fig. 1. Morphological and growth characterization of hBMCs and hPDCs. (**A**) Growth curves of hBMCs (human bone marrow-derived cells) and hPDCs (human periosteum-derived cells) over 2 weeks in culture. (**B**) Phase contrast images of hBMCs and hPDCs at one day after seeding at 5 k/cm^2, 25 k/cm^2, and 85 k/cm^2 (scale bar = 100 μm). White arrowheads indicate flattened morphology whereas black arrowheads indicate spindle-shaped morphology. (**C**) Growth kinetics of hBMCs (2 donors/2 experiments) and hPDCs (4 donors) seeded at different densities from passage 4. All error bars indicate standard error of the mean (n=3 hBMC donors or 4 hPDC donors).

25 k/cm^2, both cell types arranged in a nearly confluent, but not densely packed, monolayer of cells in which cells remained well spread against the substrate but also displayed augmented cell–cell contact. At 85 k/cm^2, both cell types appeared smaller, highly packed, and extended processes over each other (Fig. 1B), but a significant number of hBMCs did not attach after seeding at 85 k/cm^2. Because differentiation experiments last one to two weeks, we quantified the extent to which cell proliferation affected cell density over time at the different seeding densities. hBMCs seeded at 5 k/cm^2 or 25 k/cm^2 reached a cell density of 35 k/cm^2 (±2.6 k/cm^2) and 41 k/cm^2 (±4.1 k/cm^2), respectively, whereas hPDCs at those seeding densities expanded to 55 k/cm^2 (±5 k/cm^2) and 64 k/cm^2 (±4.6 k/cm^2). Cell density did not change over time for both cell types when seeded at 85 k/cm^2, though fewer hBMCs than hPDCs attached at this density (Fig. 1C).

Seeding density modulates multipotent differentiation in both hPDCs and hBMCs

To test whether seeding density modulates differentiation, hBMCs and hPDCs were seeded at 5 k/cm^2, 25 k/cm^2, and 85 k/cm^2 and subsequently treated with chondrogenic, adipogenic, or osteogenic media. Regardless of seeding density, cells cultured exclusively in growth medium did not undergo differentiation, as determined by upregulation of markers for the various lineages (data not shown). For chondrogenic differentiation, cells were plated as both monolayer and as micromass cultures (400 k cells/20 µl droplet). Micromass pellet cultures were included for comparison because it is considered to be the gold standard format for chondrogenesis. Indeed, increasing seeding density promoted expression of chondrogenic marker genes such *SOX9* (Fig. 2A), and collagen type IIa1 (*COL2A1*) (Fig. 2B) for both cell types with the highest levels of gene expression in the micromass cultures. Interestingly, *COL2A1* expression was significantly higher in hPDCs as compared to hBMCs, suggesting that hPDCs may be more prone to chondrogenic differentiation than hBMCs. Of note, cells seeded in monolayer at 85 k/cm^2 detached from tissue culture plastic after three days of treatment with chondrogenic medium. This seeding condition was therefore omitted from further analysis for chondrogenic assays (data not shown).

Increasing seeding density also promoted adipogenic differentiation of both cell types (Fig. 2C–F). After two weeks of treatment, all conditions displayed lipid droplets that stained positive for Oil Red O (Fig. 2C; insets display higher magnification of lipid droplets within differentiated cells). Quantification of Oil Red O positive cells demonstrated an increased number of adipogenic cells at 85 k/cm^2 as compared to 5 k/cm^2 for both cell types. However, there was a tenfold higher efficiency of adipogenic differentiation in hBMCs versus hPDCs (Fig. 2D). Similar results were obtained when measuring gene expression of *PPARG2*, a key transcription factor for adipogenic differentiation (Fig. 2E). Transcription of lipoprotein lipase (*LPL*), an enzyme involved in lipid metabolism, was upregulated by increased seeding density in hBMCs but not in hPDCs (Fig. 2F).

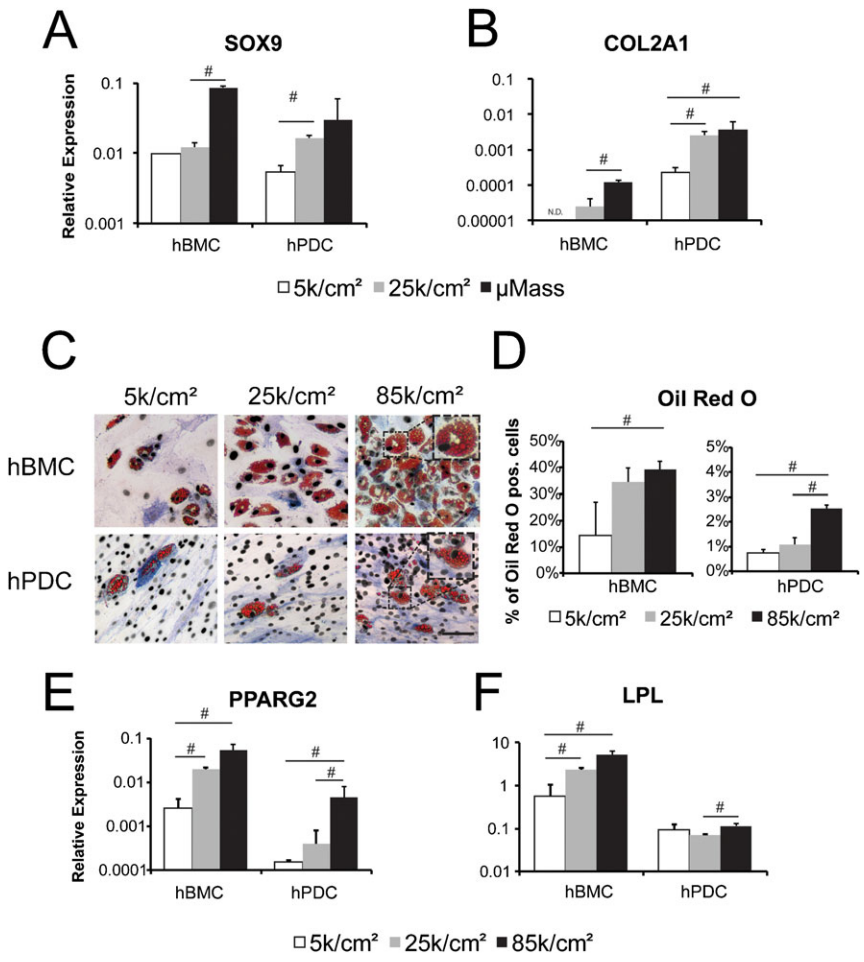

Fig. 2. Chondrogenic differentiation and adipogenic differentiation are modulated by cell seeding density in hPDCs and hBMCs. Gene expression of *SOX9* (**A**) and *COL2A1* (**B**), relative to *GAPDH* expression, in hBMCs and hPDCs seeded at 5 k/cm^2, 25 k/cm^2, or as a micromass (µMass, 400 k/20 µl) and stimulated for 14 days with chondrogenic medium. (**C**) Oil Red O staining of hBMCs and hPDCs seeded at indicated cell densities and treated for two weeks with adipogenic medium (scale bar = 100 µm). (**D**) Quantification of Oil Red O (ORO) positive cells relative to total cells as indicated by DAPI nuclear staining. Gene expression of *PPARG2* (**E**) and *LPL* (**F**), relative to *GAPDH* expression, for hBMCs and hPDCs seeded at the indicated cell densities and cultured for two weeks in adipogenic medium. Relative gene expression values are shown as $2^{-\Delta CT}$ (where ΔCT = CT value for Gene of interest − CT value for GAPDH). All error bars indicate standard deviation (n=3, #: $p \leq 0.05$, unpaired two-tailed t-test).

Unlike chondrogenesis and adipogenesis, the comparisons between hBMCs and hPDCs with respect to osteogenic differentiation were less clear. First, osteogenic medium induced transient alkaline phosphatase (ALP) activity in hBMCs by one week after stimulation, whereas two weeks of osteogenic induction were required to induce ALP activity in hPDCs (Fig. 3A). This difference in ALP kinetics between hBMCs and hPDCs is in line with previous reports (Chai et al., 2011; Eyckmans and Luyten, 2006; Jaiswal et al., 1997). Second, hBMCs but not hPDCs displayed spontaneous ALP activity in growth medium when seeded at high density. Third, seeding hBMCs but not hPDCs at 25 k/cm^2 resulted in more ALP positive cells (Fig. 3B) and increased mineralization (Fig. 3A) as compared to seeding at 5 k/cm^2. These findings at the level of protein activity were further supported by gene expression analysis for the osteogenic markers *RUNX2*, *ALP*, and osteocalcin (*OCN*). After two weeks of stimulation with osteogenic medium, hBMCs plated very densely at 85 k/cm^2 displayed higher levels of *RUNX2* and *OCN* in comparison with lower seeding densities, whereas *ALP* gene expression peaked at one week in the intermediate seeding density 25 k/cm^2 condition (Fig. 3C). By the third week, extensive calcification of the cell-secreted matrix prevented efficient RNA extraction from hBMCs (data not shown). In contrast to hBMCs, seeding density did not affect expression of the osteogenic marker genes in hPDCs during the first two weeks of stimulation. By three weeks after stimulation, however, hPDCs seeded at low density tended to express higher mRNA levels of *ALP* and *OCN* (Fig. 3C). The absence of an effect of cell density on *RUNX2* and the relatively mild effect on *ALP* and *OCN* expression in hPDCs suggest that osteogenic differentiation in hPDCs may be less sensitive than the hBMCs to cues affected by cell density.

Seeding density affects cell shape of hPDCs and hBMCs

The augmented differentiation response observed at higher seeding densities could be attributed to multiple co-varying factors that inevitably change when increasing the number of cells in a culture vessel, such as cell-extracellular matrix adhesion, cell–cell contact, paracrine signaling, and cell shape. In contrast to epithelial cells that form a monolayer upon full

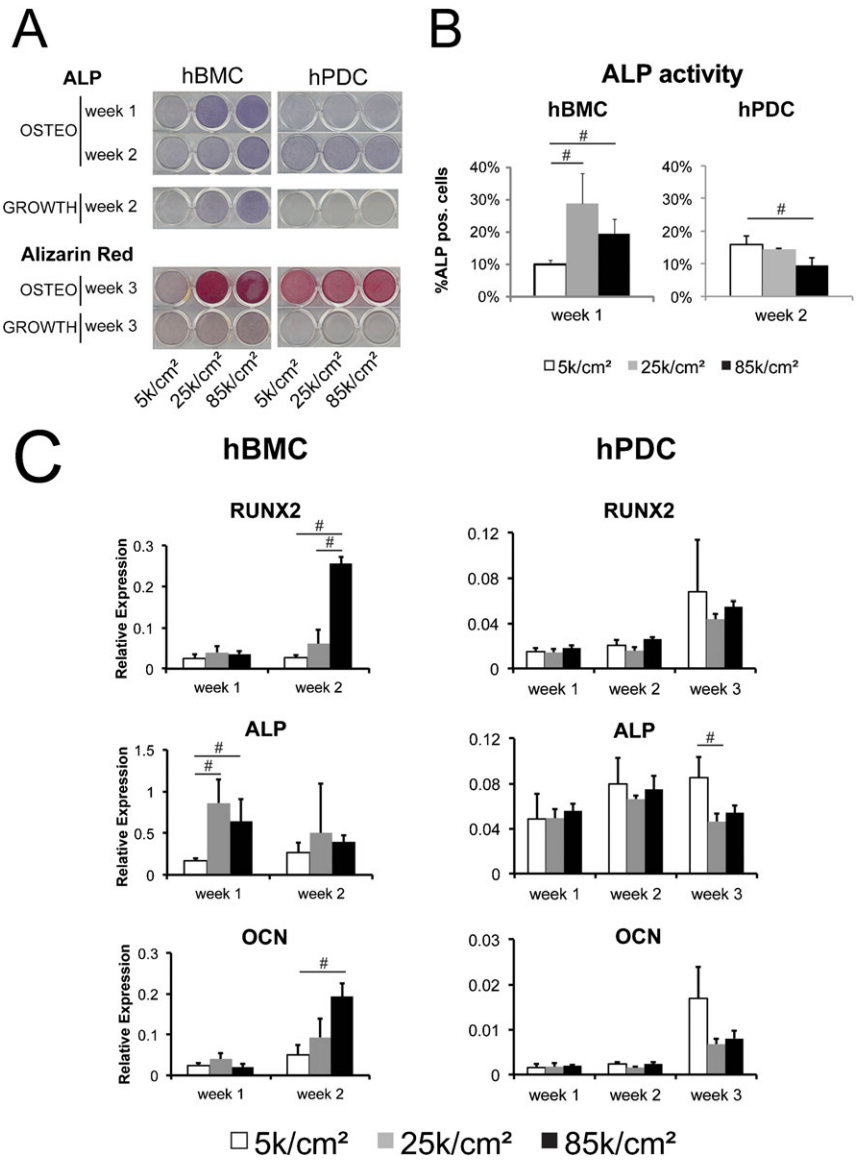

Fig. 3. Cell seeding density affects osteogenic differentiation. (**A**) Enzymatic staining of alkaline phosphatase (ALP) in hBMCs and hPDCs seeded at the indicated cell densities and treated with osteogenic or growth medium for 1 and 2 weeks or stained for mineralization with alizarin red after 3 weeks of osteogenic stimulation or growth medium. (**B**) Quantification of ALP positive cells relative to total cells shown at the indicated timepoints, which differ due to distinct ALP kinetics between these two cell types. (**C**) Gene expression of the bone markers, *RUNX2*, *ALP*, and osteocalcin (*OCN*), all relative to the expression of *GAPDH*, for hBMCs and hPDCs seeded at the indicated cell densities and cultured for the indicated duration in osteogenic medium. By the third week of hBMC culture, extensive calcification of the cell-secreted matrix prevented efficient RNA extraction despite repeated attempts (data not shown). All error bars indicate standard deviation (n=3, #: $p \leq 0.05$, unpaired two-tailed t-test).

confluency, primary MSCs can expand on top of each other, giving rise to multilayered cell sheets. By consequence, the surface area to which a cell can adhere is not exclusively restricted by the number of seeded cells. To gain insight into how seeding density impacts cell shape in hPDCs and hBMCs, we tagged a fraction of the cells with cytoplasmic GFP and mixed them with non-fluorescent cells prior to seeding at different cell densities. The next day, the medium was replaced by growth, osteogenic, or adipogenic medium for two more days. Measurements of projected area of cells at 20 hours after seeding confirmed our initial observation that hPDCs were less spread than hBMCs when seeded at 5 k/cm^2, and that cell area was significantly reduced in conditions seeded at 25 k/cm^2 (hBMCs) and 85 k/cm^2 (hBMCs and hPDCs) (Fig. 4A,B). Furthermore, spread area remained inversely correlated with initial seeding density up to day 3. For both cell types, the variability in cell size was consistently reduced at high seeding densities (Fig. 4B,C), suggesting that cell shape is more homogenous in high cell density cultures. In addition to the effects of seeding density on cell area, treatment with adipogenic medium also reduced cell area at higher seeding densities (Fig. 4C), demonstrating that cell shape is in part regulated by soluble factors.

Cell shape regulates differentiation of both hPDCs and hBMCs

Because cell shape appeared to be influenced by cell density, we utilized fibronectin micropatterning techniques to directly assess the impact of cell shape on MSC differentiation without the complex effects of seeding density. Briefly, 25μm×25μm (625 μm^2) or 100μm×100μm (10000 μm^2) fibronectin islands were stamped on a polydimethylsiloxane surface, followed by seeding of hBMCs and hPDCs. We used smaller fibronectin patterns (625 μm^2) here than previously utilized for hBMCs (1024 μm^2) (Gao et al., 2010; McBeath et al., 2004) since hPDCs are smaller than hBMCs (Fig. 4B). Cells that adhered to 625 μm^2 fibronectin islands adopted a round, unspread cell shape, while the cells on the larger fibronectin patterns were able to spread out to a surface area of 10000 μm^2 (Fig. 5A). As such cell shape is altered without modulating seeding density.

Under these conditions, treatment of hBMCs and hPDCs with chondrogenic medium for two weeks resulted in an increased percentage of cells that stained positive for collagen type II when adherent on small 625 μm^2 versus large 10000 μm^2 islands (Fig. 5A). Similarly, hBMCs seeded on small patterns versus large patterns displayed higher levels of mRNA expression for the chondrogenic marker *SOX9* (Fig. 5B). Although a similar trend was observed in hPDCs for *COL2A1*, the effect was not significant due to the high variability between experiments. *COL2A1* expression in hBMCs was only detected in small patterned cells in one of four experiments (Fig. 5B). These micropatterned data show that chondrogenic gene expression in hPDCs appears to be less regulated by cell shape than that in hBMCs, whereas chondrogenic expression at the protein level is similarly regulated by shape in both cell types. Thus the promotion of chondrogenic gene expression by increased cell density in hPDCs may be more heavily influenced by density-induced cues other than cell spreading, such as increased cell–cell signaling. Nonetheless, the trend toward improved

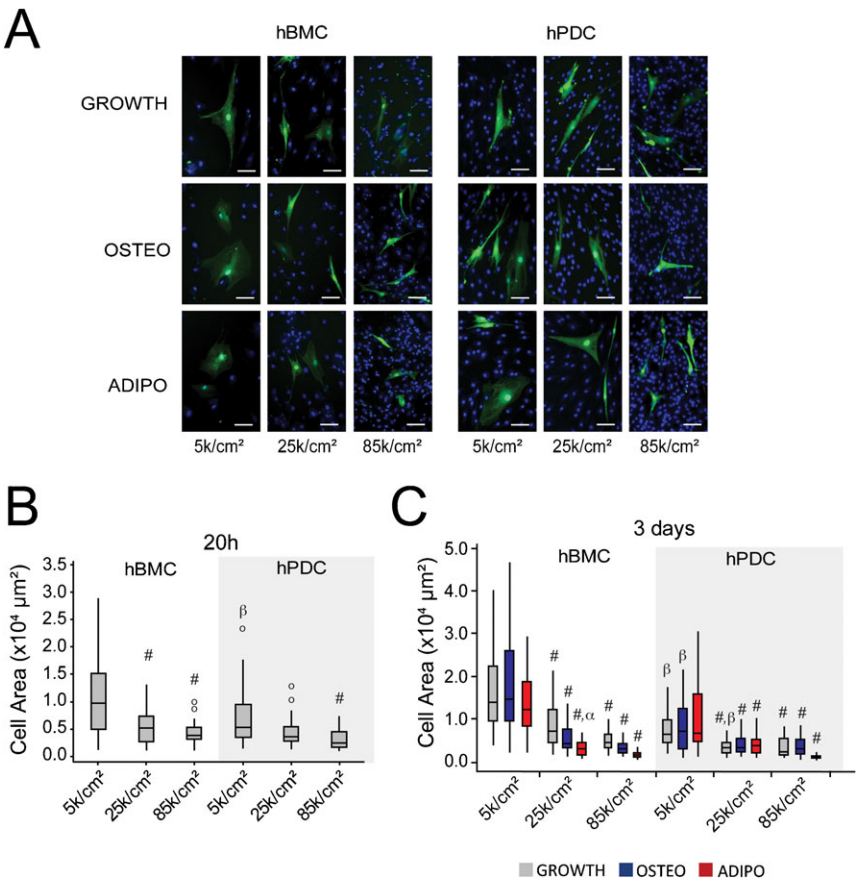

Fig. 4. Seeding density modulates cell shape in both cell types. (**A**) Fluorescent microscopy images of GFP-labeled hBMCs and hPDCs mixed with unlabeled cells and seeded at different densities. Images are taken 3 days after seeding in presence of osteogenic (OSTEO) or adipogenic (ADIPO) differentiation medium for the last 2 days, or growth medium (GROWTH) for all 3 days (Green: GFP, Blue: DAPI counterstained nuclei, scale bar = 100 μm). (**B**) Quantification of cell spread area for GFP-labeled hPDCs and hBMCs at 20 hours after seeding (#: $p \leq 0.05$, comparing to 5 k/cm^2 condition; β: $p \leq 0.05$, comparing to hBMCs seeded at the same density; o: outliers). (**C**) Quantification of cell spread area at 3 days after seeding (#: $p \leq 0.05$, comparing to 5 k/cm^2 condition in the same medium, α: $p \leq 0.05$, comparing to the same seeding condition in growth medium, β: $p \leq 0.05$, comparing to hBMCs under the same seeding/medium conditions. 30–60 cells were counted per condition. Statistical significance calculated by ANOVA and Tukey's post hoc test).

chondrogenesis in small versus large patterns still suggests some contribution of cell spreading to the observed increase in chondrogenesis with high seeding densities.

Comparable to chondrogenesis, directly restricting cell spreading also promoted adipogenic differentiation. The percentage of Oil Red O positive hBMCs and hPDCs was higher in cells constrained on small fibronectin islands as compared to cells patterned on large islands (Fig. 5C). These data were supported by gene expression analysis of *PPARG2* and *LPL*, which tended toward higher levels of expression in unspread as compared to spread hBMCs (Fig. 5D). Although similar trends were obtained for unspread and spread hPDCs within single experiments, there was considerable variability across experiments (Fig. 5D).

In contrast to the adipogenic and chondrogenic lineages, the osteogenic marker *ALP* was expressed at lower levels in unspread

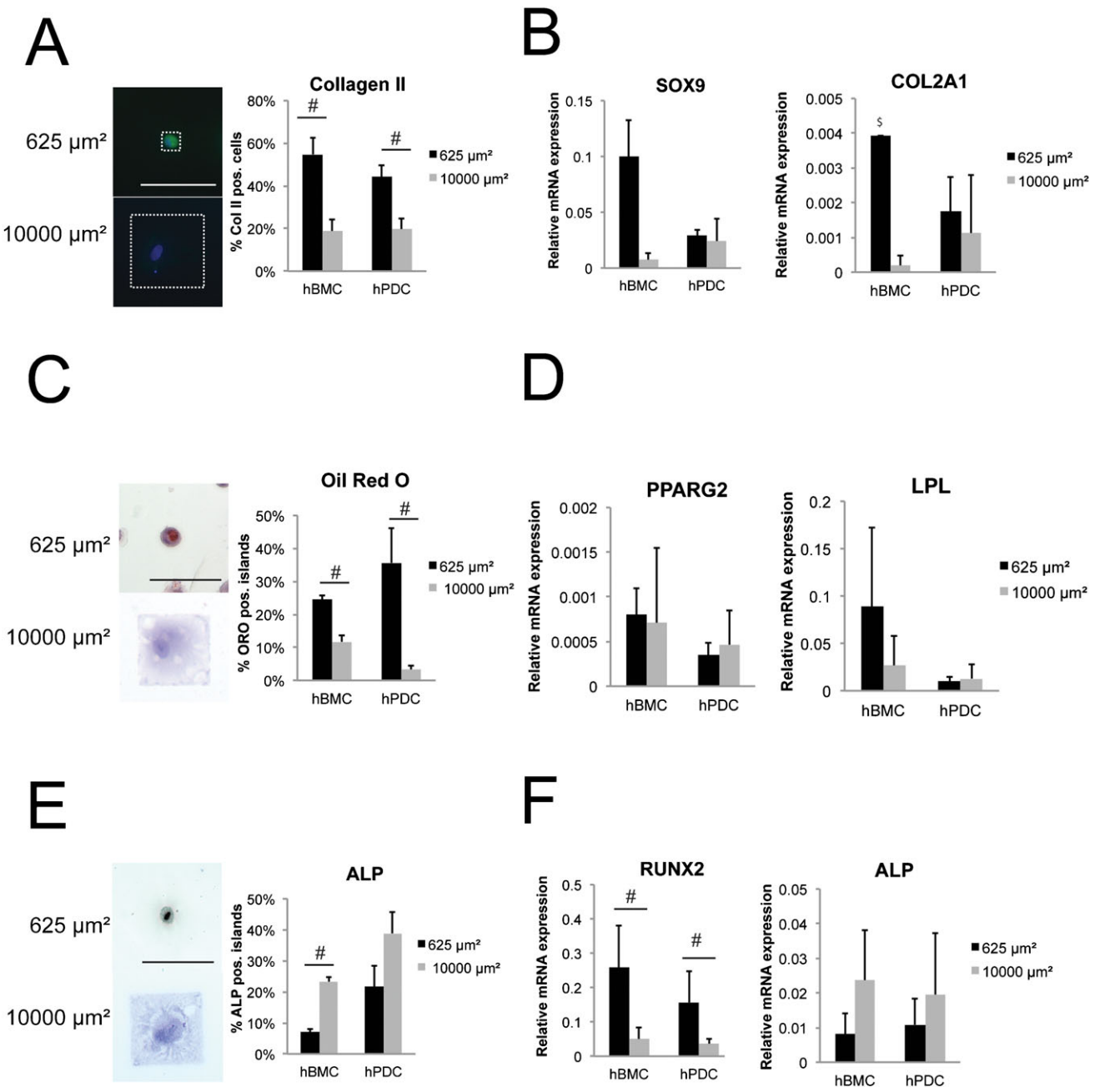

Fig. 5. Cell shape controls differentiation in hPDCs and hBMCs. Chondrogenic (**A**,**B**), adipogenic (**C**,**D**), and osteogenic (**E**,**F**) differentiation of hBMCs and hPDCs patterned on 625 µm^2 or 10000 µm^2 fibronectin islands and cultured in the indicated medium for 2 weeks. A,C,E show representative cell images and quantification of cells staining positive for (A) collagen type II (green: Collagen II, blue: DAPI counterstaining), (C) Oil Red O (hematoxylin counterstaining), and (E) ALP. White dashed box in (A) outlines one 625 µm^2 and one 10000 µm^2 fibronectin pattern (scale bar = 100 µm). Gene expression of markers indicative for chondrogenesis (B, *SOX9* and *COL2A1*), adipogenesis (D, *PPARG2* and *LPL*), and osteogenesis (F, *ALP* and *RUNX2*), expressed relative to *GAPDH*. All error bars indicate standard error of the mean (n=2 hBMC donors or 4 hPDC donors; n=3–6 independent experiments per lineage; $: result obtained in only one experiment). (#: $p \leq 0.05$, Mann-Whitney U test for A–E, unpaired two-tailed t-test for F).

versus spread cells. When spread on large fibronectin islands, more hBMCs and hPDCs displayed ALP activity (Fig. 5E) and increased *ALP* gene expression (Fig. 5F) as compared to size-restricted cells. However, cells adherent to small patterns showed significantly higher levels of *RUNX2* mRNA transcripts (Fig. 5F). As *RUNX2* is an earlier marker of osteogenesis than ALP (Otto et al., 1997), these findings are consistent with a possibility that different degrees of cell spreading may be optimal for different stages of differentiation. Interestingly, the observation that increased cell spreading enhanced *ALP* expression via micropatterning, and that increasing cell seeding density (which decreases cell spreading) either enhanced (hBMCs) or decreased *ALP* expression (hPDCs), suggests that increased hBMC seeding density introduces an additional pro-osteogenic cue that is independent of cell shape.

Impaired RhoA/ROCK signaling affects differentiation of hPDCs

Because changes in cell shape alter cytoskeletal tension and RhoA/Rho Kinase (ROCK) activity (Bhadriraju et al., 2007; McBeath et al., 2004), it has been hypothesized that RhoA/ROCK signaling may regulate MSC differentiation. Indeed, we have previously demonstrated in hBMCs that manipulation of RhoA/ROCK signaling modulates osteogenic versus adipogenic commitment when cells are treated with a mixed osteogenic/adipogenic stimulation medium (McBeath et al., 2004). In addition, hBMC osteogenesis is inhibited by treatment with the ROCK inhibitor Y27632 (Wang et al., 2011). Others have shown that RhoA/ROCK signaling also regulates chondrogenic differentiation in adipose tissue-derived MSCs (Lu et al., 2010) and gingiva-derived MSCs (Hsu et al., 2012). No data have yet been reported, however, regarding a role for RhoA/ROCK signaling in hPDCs. Here we examined whether inhibition of RhoA/ROCK signaling, by addition of the ROCK inhibitor Y27632, alters osteogenic, adipogenic, and chondrogenic differentiation in hPDCs seeded at low and high density.

Y27632 treatment caused micromasses to remain adherent to tissue culture plastic as compared with non-treated controls indicating drug efficacy (Fig. 6A, bright field image inset). However, Y27632 treatment did not significantly influence chondrogenic differentiation for any conditions as measured by alcian blue uptake, even though measurements trended toward significance for Y27632-treated micromasses (Fig. 6A). At the gene expression level, chondrogenesis for hPDCs seeded as micromasses was modestly enhanced by Y27632 treatment, but not for hPDCs seeded at low density (Fig. 6B).

For adipogenesis, Y27632 treatment increased the percentage of Oil Red O positive cells (Fig. 6C) and upregulated gene transcription of *PPARG2* and *LPL* (Fig. 6D) in hPDCs seeded at low density. The additional fraction of lipid droplet-forming adipogenic cells induced by Y27632 at low seeding density did not reach the level of adipogenic cells without Y27632 at high seeding density. These trends did not reach statistical significance for cells seeded at high density.

In contrast, ALP activity (Fig. 6E) and *ALP* and *RUNX2* gene expression (Fig. 6F) were significantly downregulated in the presence of Y27632 for hPDCs seeded at low density. In hPDCs seeded at high density, osteogenic gene expression but not ALP activity was suppressed by Y27632. Interestingly, Y27632 treatment even in osteogenic differentiation medium resulted in a small but detectable number of cells that produced lipid droplets staining positive for Oil Red O (supplementary material Fig. S1). These results in hPDCs are consistent with reports of Y27632-induced effects on mesenchymal differentiation in hBMCs (McBeath et al., 2004), suggesting that cytoskeletal tension-mediated regulation of differentiation is conserved for hPDCs. Of note, addition of Y27632 did not significantly affect proliferation of hPDCs cultured in any of the differentiation media as compared to untreated controls over the duration of the differentiation experiments (data not shown), indicating that Y27632 was not toxic to the cells.

Discussion

Cells undergo dynamic changes in cell shape during embryonic morphogenesis *in vivo* (Mammoto and Ingber, 2010), but only recently have scientists had the tools to manipulate cell shape *in vitro*, for instance by micropatterning (Eyckmans et al., 2011). With the ability to test the hypothesis *in vitro* that cell shape influences stem cell fate, we and other groups have recently demonstrated that cell shape can modulate the multipotential lineage commitment of hBMCs (Gao et al., 2010; Kilian et al., 2010; McBeath et al., 2004). Micropatterned hBMCs in mixed osteogenic/adipogenic media give rise to either fate depending on the initial spread cell area, and contractility inhibitors promote "round" cell fates like adipogenesis while inhibiting osteogenic differentiation (McBeath et al., 2004). In addition, increases in cell density impose physical constraints on cell shape, leading to decreased projected cell area (McBeath et al., 2004; Nelson and Chen, 2002; Xu et al., 2010). In this study, we extend these findings to hPDCs and show that differentiation efficiency in hBMC and hPDC populations can be guided by changing seeding density or cell shape. In both cell types, increasing cell seeding density or reducing cell spreading yielded better adipogenic and chondrogenic differentiation. In addition, the effect of inhibiting RhoA/ROCK signaling in hPDCs partially mimicked cell density/shape dependent differentiation effects, which is consistent with what has already been published for hBMCs (Gao et al., 2010; McBeath et al., 2004; Wang et al., 2011). Moreover, this study is in line with prior work suggesting that ROCK acts downstream of the effects of cell shape on differentiation (McBeath et al., 2004), since despite the fact that Y27632 induces a differentiation phenotype of a less spread cell, morphologically Y27632 either does not impact cell shape or enhances cell spreading.

Interestingly, while our data showed consistent trends for regulation of chondrogenic and adipogenic differentiation by cell adhesion, shape, and mechanics in both hBMCs and hPDCs, mechanoregulation of osteogenic differentiation was more complex. Increasing seeding density significantly decreased (hPDCs) or increased (hBMCs) the fraction of MSCs expressing active ALP protein, but ALP gene expression and protein activity were higher in MSCs on spread versus small patterns. Because higher cell density not only decreased cell spreading, but also would be expected to increase the level of paracrine (diffusible) and juxtacrine (cell–cell contact) signaling from neighboring cells, these data suggest the presence of a pro-osteogenic signal with increasing seeding density that opposes and masks the underlying spreading-dependent osteogenic signal. That is, the biomechanical effect of cell spreading on promoting osteogenic differentiation may be concealed by pro-osteogenic cell–cell signaling effects in high density cultures but exposed by the micropatterned cultures. Cell type-specific differences in sensitivity to this phenomenon may explain why osteogenesis

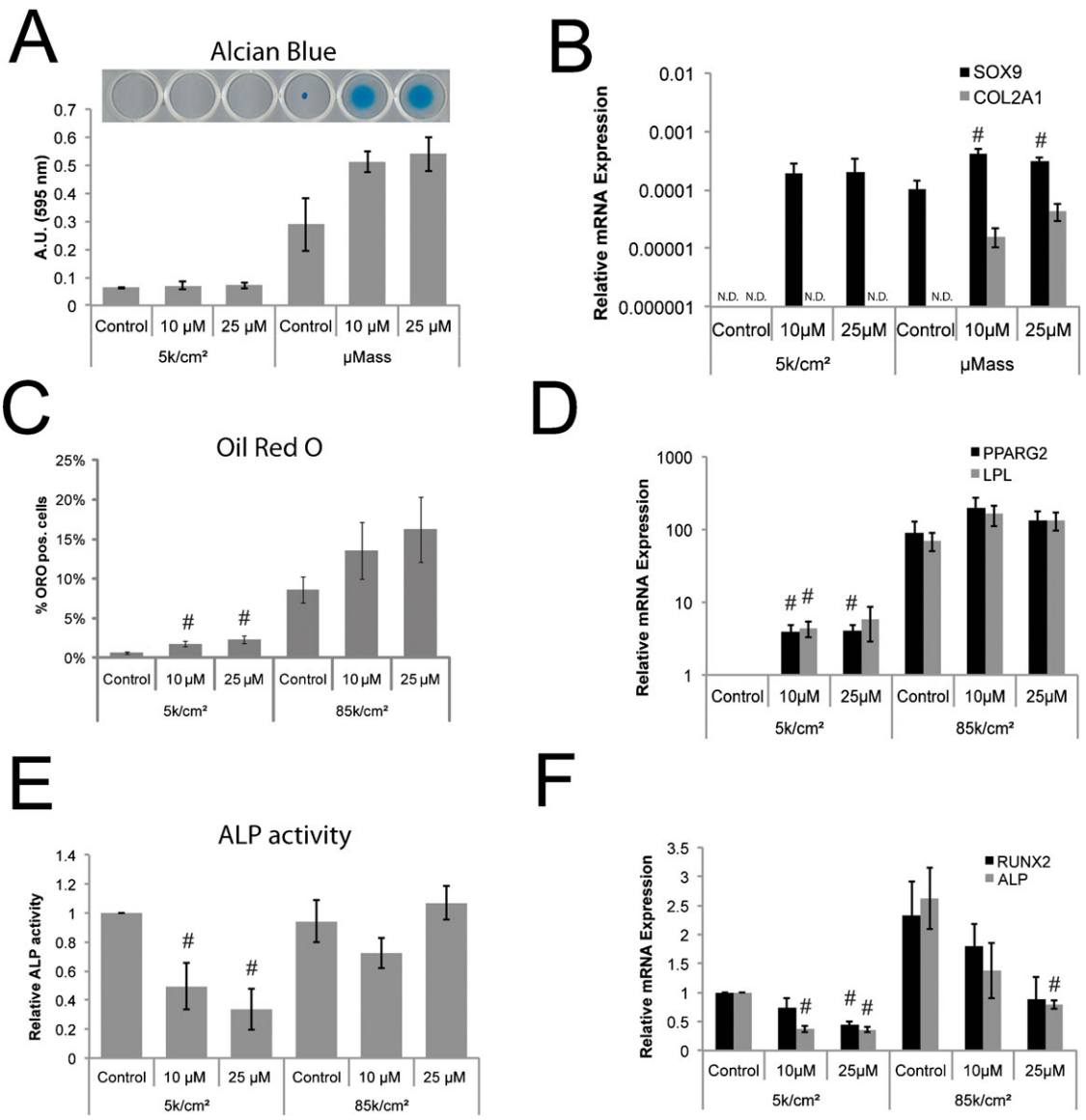

Fig. 6. Inhibition of RhoA/ROCK signaling promotes adipogenesis and chondrogenesis but inhibits osteogenesis in hPDCs. Chondrogenic (**A**,**B**), adipogenic (**C**,**D**), and osteogenic (**E**,**F**) differentiation of hPDCs seeded at 5 k/cm^2 or as a micromass (μMass, 400 k/20 μl) (A,B), or at 85 k/cm^2 (C–F), and cultured for 2 weeks in chondrogenic, adipogenic, or osteogenic medium containing no drug (control) or the ROCK inhibitor Y27632 at 10 or 25 μM. A,C,E display quantification of cells staining positive for (A) alcian blue, (C) Oil Red O, and (E) ALP. (A) also shows representative alcian blue staining images, demonstrating that Y27632 treatment improved micromass adherence. Relative gene expression ($2^{-\Delta CT}$ with ΔCT=(CT value for Gene of interest−CT value for GAPDH)) of differentiation markers indicative for chondrogenesis (B, *SOX9* and *COL2A1*), or $2^{-\Delta\Delta CT}$ as normalized to the 5 k/cm^2 control condition for adipogenesis (D, *PPARG2* and *LPL*) and osteogenesis (F, *ALP* and *RUNX2*). All error bars indicate standard error of the mean (#: $p \leq 0.05$, comparing to control condition for the same seeding condition; unpaired two-tailed t-test for n=4 hPDC donors; N.D.: not detected or result obtained in only one experiment).

in hPDCs was less affected by cell density manipulations than in hBMCs, while both cell types responded to differences in spread cell area through micropatterning. In addition, we observed that confining hPDCs on small fibronectin islands yielded a higher percentage of adipogenic differentiation in comparison to hPDCs with the same spread area in high density cultures, suggesting that these paracrine/juxtacrine signals also suppress hPDC adipogenesis. Paracrine signaling may also strongly influence chondrogenic differentiation in hPDCs, since chondrogenic gene expression was promoted by high density cultures to a greater degree than by small, unspread patterned cultures. Indeed, paracrine signals have been shown to impact differentiation. For instance, changes in paracrine PDGF signaling can modulate the cardiomyogenic potential of mouse BMCs (Pallante et al., 2007). In another study using a microfluidic platform designed to continuously wash away cell-secreted factors, investigators found a requirement for paracrine signaling in mouse embryonic stem cells committing to the neuroectodermal lineage (Blagovic et al., 2011). Hence increased cell density may partially mediate differentiation effects by enhancing paracrine signaling, via both the greater numbers of cells able to secrete signaling factors and the decreased diffusion distance between neighboring cells. In fact, a critical mass of MSCs in osteogenic scaffolds is required for bone formation to occur *in vivo* (Eyckmans et al., 2010; Mankani et al., 2007), indicating that cell–cell signaling is indispensible in certain differentiation assays. Our results show

that effects of both shape and cell–cell signaling are important for chondrogenesis and osteogenesis in hPDCs, suggesting that these cues are relevant to cartilage and bone formation and repair. These findings are consistent with literature showing that hPDCs implanted at high cell density, but not low density, *in vivo* appear to pass through an early chondrogenic phase (Nakahara et al., 1991b).

It is clear from our data and other reports, however, that differences in cell shape can affect differentiation independently of cell–cell contact. The mechanisms by which cell shape regulates MSC differentiation and other cell behaviors remain to be elucidated. There is mounting evidence for the involvement of focal adhesion signaling and cytoskeletal tension as key factors. Focal adhesions serve dual functions as biophysical anchorage points between the cytoskeleton and the extracellular matrix and as active signaling sites. Altering adhesive conditions may influence the availability or activity of various signaling molecules that localize to adhesions and have been implicated in differentiation, including FAK, Src, β-catenin, and MAPK proteins, among others (Blagovic et al., 2011; Kuo et al., 2011; Miyamoto et al., 1995; Schiller et al., 2011). Additionally, focal adhesion maturation is correlated with increased RhoA-mediated cytoskeletal tension and the formation of stress fibers (Ridley and Hall, 1992; Riveline et al., 2001), both of which contribute to cell shape (Chen et al., 2003; Tan et al., 2003). Inhibition of cytoskeletal tension via drugs like the ROCK inhibitor Y27632 has been reported to regulate mesenchymal differentiation in hBMCs and adipose-derived MSCs (Lu et al., 2010; McBeath et al., 2004; Wang et al., 2011; Xu et al., 2010). Similarly in our experiments, treatment of hPDCs with Y27632 promoted adipogenic differentiation but reduced osteogenic differentiation. Although cytoskeletal tension is required for stabilization of adhesions, it also impacts cellular signaling at the transcriptional level. Actomyosin-mediated contractility regulates nucleocytoplasmic transport of mRNA binding proteins (Lee et al., 2004; Oleynikov and Singer, 2003) and transcription factors such as Yes-associated protein (YAP) and transcriptional coactivator with PDZ binding motif (TAZ), both of which are involved in osteogenic/adipogenic differentiation (Dupont et al., 2011). Actin polymerization also drives nuclear localization of serum response factor (SRF) and its co-factor myocardin-related transcription factor (MRTF) (Vartiainen et al., 2007), which can drive terminal differentiation of epidermal stem cells (Connelly et al., 2010) and epithelial-mesenchymal transition (Gomez et al., 2010). Thus cytoskeletal tension and mechanochemical signaling at adhesions contribute to the role of cell shape in regulation of stem cell differentiation.

Taken together, these studies suggest that mechanoadhesive regulation of differentiation extends beyond hBMCs to hPDCs, and that this process likely plays a role in many if not all MSCs. As such, adhesive and mechanical cues will need to be optimized for each MSC source in order to fairly compare differentiation of different stem cells. For instance, in our experiments, the best condition for adipogenic differentiation of hBMCs was at high seeding density, whereas hPDC adipogenic commitment was better on small micropatterns with minimized cell–cell signals. Another example is that because hPDCs are smaller and spread less than hBMCs, the seeding densities and micropattern area that impacted differentiation were shifted. Thus, the general mechanisms by which biophysical cues regulate behavior may be conserved across different stem cells, but the relative importance and optimal conditions may differ for each cell type. Given this, comparison studies between cell types should carefully control for and describe biophysical parameters for accurate replication in future work, which may also reduce some of the reported variability in MSC differentiation studies.

Materials and Methods

Cell culture and assessment of growth curves

hBMCs from two donors were purchased from Lonza (Walkersville, MD, USA) and expanded in Dulbecco's Modified Eagle Medium (DMEM, 1 g/L glucose; Mediatech Inc, Manassas, VA, USA) supplemented with 10% Fetal Bovine Serum (FBS) (Atlanta Biologicals, Lawrenceville, GA, USA). hPDCs were isolated from four patients and expanded in growth medium (DMEM, 4.5 g/L glucose + 10% FBS) as described previously (Eyckmans et al., 2010). In brief, periosteal biopsies were harvested from the proximal tibia of male and female patients (mean: 26 (±14) years of age), digested in collagenase (Invitrogen, Grand Island, NY, USA) in growth medium, collected by centrifugation, and seeded in a T25 flask in growth medium. Non-adherent cells were removed after 5 days by changing the medium. The ethical committee for Human Medical Research (Katholieke Universiteit Leuven) approved all procedures, and patient informed consent forms were obtained.

To establish growth curves, hBMCs and hPDCs were seeded in 12 well plates at 5 k/cm^2. At different time points, cells were stained with DAPI and imaged with a SPOT CCD camera (Diagnostic Instruments, Sterling Heights, MI, USA) mounted on a Nikon TE200 microscope at 100× magnification. Nuclei were counted with Cell Profiler (Carpenter et al., 2006).

Cell shape analysis

To assess cell shape, cells infected with a lentiviral vector encoding for enhanced Green Fluorescent Protein (eGFP) were mixed with non-infected cells and seeded at 5 k/cm^2, 25 k/cm^2, or 85 k/cm^2 in growth medium. The next day, the cultures were imaged at 100× and medium was changed to either growth medium, osteogenic, or adipogenic medium (Lonza). Two days later, GFP-positive cells were imaged and analyzed in ImageJ (Abramoff et al., 2004). For each condition, 30 to 60 cells were manually outlined and projected cell area was measured.

Fibronectin micropatterning

To control cell shape, 25μm×25μm (625 μm^2) or 100μm×100μm (10000 μm^2) adhesive islands of fibronectin were stamped on Polydimethylsiloxane (PDMS) (Dow Corning Sylgard 184, Midland, MI, USA) substrates as described previously (Tan et al., 2002). Briefly, glass coverslips were spin-coated with PDMS, baked to cure the PDMS, cleaned in 70% ethanol, rinsed with PBS, and treated with UV-ozone (UVO Cleaner, Jelight Company Inc, Irvine, CA, USA) for 5 minutes. Fibronectin (BD Biosciences, San Jose, CA, USA) was loaded on PDMS positive-featured stamps at 50 μg/ml for 1 hour, rinsed in sterile water, dried with a nitrogen gun, and stamped onto the PDMS-glass substrates. Subsequently, the stamped substrates were blocked with pluronic F127 (BASF, Mt. Olive, NJ, USA) to prevent cell attachment outside the fibronectin islands, and rinsed with PBS several times before cell seeding.

Differentiation assays

For differentiation assays, passage 4 to passage 7 cells were seeded in 24 or 12 well plates at 5 k/cm^2, 25 k/cm^2, 85 k cells/cm^2, in micromasses (400 k cells in a 20 μl droplet), or on patterned fibronectin substrates; all in growth medium (DMEM + 10% FBS (Atlanta Biologicals, Lawrenceville, GA, USA). After 24 hours, the medium was replaced with osteogenic, adipogenic, or chondrogenic induction media (Lonza Poetics™: hMSC Osteogenic Differentiation BulletKit™ (osteo basal medium, dexamethasone, ascorbate, mesenchymal cell growth supplement, L-glutamine, penicillin, streptomycin, β-glycerophosphate), hMSC Adipogenic Differentiation BulletKit™ (adipo basal medium, indomethacin, isobutylmethylxanthine, recombinant human insulin, dexamethasone, GA-1000 (gentamicin, amphotericin B), mesenchymal cell growth supplement, L-glutamine), or hMSC Chondrogenic Differentiation BulletKit™ [chondro basal medium, dexamethasone, ascorbate, ITS+ supplement (insulin, human transferrin, selenous acid), pyruvate, proline, GA-1000, L-glutamine) supplemented with 10 ng/ml TGFβ1 (StemRD, Burlingame, CA, USA)]. Differentiation induction media were changed every other day for up to three weeks unless otherwise stated. To reduce cytoskeletal tension during differentiation, a Rho Kinase (ROCK) inhibitor, Y27632 (Tocris Bioscience, R&D systems Inc, Minneapolis, MN, USA), was added to differentiation medium at a final concentration of 10 μM or 25 μM.

Staining

Cells were fixed with 4% paraformaldehyde (Electron Microscopy Sciences, Hatfield, PA, USA) and stained for alkaline phosphatase with Fast Blue RR Salt/naphthol (Sigma–Aldrich, St. Louis, MO, USA), lipid droplets with Oil Red O

(Sigma–Aldrich) in 60% isopropanol, and nuclei with DAPI or hematoxylin. Highly sulphated mucins, characteristic for cartilage-like matrix, were stained with alcian blue 8GX (in 0.5 M HCl, pH 1.5) (Sigma–Aldrich) for 24 hours. After washing, dye bound to the matrix was extracted with 6 M guanidium chloride (Sigma–Aldrich) and absorbance was measured at 592 nm with a GENios microplate reader (Tecan, Durham, NC, USA). Mineralization was stained by Alizarin Red S (Acros Organics, Fair Lawn, NJ) as a 2% solution in water with pH adjusted to 4.2 with 10% ammonium hydroxide for 15 min followed by washes. Immunohistochemistry for collagen type II was performed with a monoclonal mouse anti-human collagen type II antibody (1:300 dilution) (MP Biomedicals, Solon, OH, USA) as a primary antibody and a goat anti-mouse alexa 488 conjugated (Invitrogen) as secondary antibody, as described previously (Gao et al., 2010).

RNA extraction and quantitative PCR

RNA was extracted with the RNA micro/minikit from Qiagen (Qiagen Sciences, Germantown, MD, USA) according to the manufacturer's protocol. Complementary DNA (cDNA) was obtained by reverse transcription of 1 µg of total RNA with qScript^{TM} cDNA Supermix (Quanta Sciences, Gaithersburg, MD, USA). Realtime PCR was performed in 20 µl reactions using the PerfeCTa^{TM} mastermix (Quanta Sciences) and a 7300 Real Time PCR System (Applied Biosystems, Foster City, CA, USA) cycling at 95℃ for 3 seconds and 60℃ for 20 seconds for 40 cycles. The following Taqman® primer/probe sets (Applied Biosystems) were utilized for marker gene expression: *RUNX2*: Hs00231692_m1, *ALP*: Hs00758162_m1; *OCN:* Hs01587814_g1; *SOX9*: Hs00165814_m1; *COL2a1*: Hs00264051_m1; *PPARG2*: Hs00234592; *LPL*: Hs00173425; *GAPDH*: Hs99999905_m1. Relative gene expression is shown either as (1) $2^{-\Delta CT}$ with ΔCT=[CT value for Gene of interest−CT value for Glyceraldehyde 3-phosphate dehydrogenase (GAPDH)] where the Gene of Interest is a differentiation marker, or (2) $2^{-\Delta\Delta CT}$ as normalized to the 5 k/cm^2 control condition in the same media condition, as detailed in each figure legend.

Statistical analysis

For each graph, the mean represents the average of three to six experiments. Statistical comparisons between experimental conditions were performed utilizing a Mann-Whitney U test or an unpaired two-tailed t-test. Cell projected areas under different density and media conditions were compared with a one-way ANOVA followed by Tukey post hoc test. For all tests, statistical significance was assigned at p-value ≤ 0.05.

Acknowledgements

This work was supported by National Institutes of Health [grant numbers GM60692, EB 00262]. J.E. is a postdoctoral fellow of the Research Foundation – Flanders (FWO).

Competing Interests

The authors have no competing interests to declare.

References

Abramoff, M. D., Magalhães, P. J. and Ram, S. J. (2004). Image Processing with ImageJ. *Biophotonics Int.* **11**, 36-42.

Agata, H., Asahina, I., Yamazaki, Y., Uchida, M., Shinohara, Y., Honda, M. J., Kagami, H. and Ueda, M. (2007). Effective bone engineering with periosteum-derived cells. *J. Dent. Res.* **86**, 79-83.

Augello, A. and De Bari, C. (2010). The regulation of differentiation in mesenchymal stem cells. *Hum. Gene Ther.* **21**, 1226-1238.

Bhadriraju, K., Yang, M., Alom Ruiz, S., Pirone, D., Tan, J. and Chen, C. S. (2007). Activation of ROCK by RhoA is regulated by cell adhesion, shape, and cytoskeletal tension. *Exp. Cell Res.* **313**, 3616-3623.

Blagovic, K., Kim, L. Y. and Voldman, J. (2011). Microfluidic perfusion for regulating diffusible signaling in stem cells. *PLoS ONE* **6**, e22892.

Boeuf, S. and Richter, W. (2010). Chondrogenesis of mesenchymal stem cells: role of tissue source and inducing factors. *Stem Cell Res. Ther.* **1**, 31.

Carpenter, A. E., Jones, T. R., Lamprecht, M. R., Clarke, C., Kang, I. H., Friman, O., Guertin, D. A., Chang, J. H., Lindquist, R. A., Moffat, J. et al. (2006). CellProfiler: image analysis software for identifying and quantifying cell phenotypes. *Genome Biol.* **7**, R100.

Chai, Y. C., Roberts, S. J., Schrooten, J. and Luyten, F. P. (2011). Probing the osteoinductive effect of calcium phosphate by using an *in vitro* biomimetic model. *Tissue Eng. Part A* **17**, 1083-1097.

Chen, C. S., Alonso, J. L., Ostuni, E., Whitesides, G. M. and Ingber, D. E. (2003). Cell shape provides global control of focal adhesion assembly. *Biochem. Biophys. Res. Commun.* **307**, 355-361.

Colnot, C. (2009). Skeletal cell fate decisions within periosteum and bone marrow during bone regeneration. *J. Bone Miner. Res.* **24**, 274-282.

Connelly, J. T., Gautrot, J. E., Trappmann, B., Tan, D. W., Donati, G., Huck, W. T. and Watt, F. M. (2010). Actin and serum response factor transduce physical cues from the microenvironment to regulate epidermal stem cell fate decisions. *Nat. Cell Biol.* **12**, 711-718.

De Bari, C., Dell'Accio, F., Vanlauwe, J., Eyckmans, J., Khan, I. M., Archer, C. W., Jones, E. A., McGonagle, D., Mitsiadis, T. A., Pitzalis, C. et al. (2006). Mesenchymal multipotency of adult human periosteal cells demonstrated by single-cell lineage analysis. *Arthritis Rheum.* **54**, 1209-1221.

Dominici, M., Le Blanc, K., Mueller, I., Slaper-Cortenbach, I., Marini, F., Krause, D., Deans, R., Keating, A., Prockop, D. and Horwitz, E. (2006). Minimal criteria for defining multipotent mesenchymal stromal cells. The International Society for Cellular Therapy position statement. *Cytotherapy* **8**, 315-317.

Dupont, S., Morsut, L., Aragona, M., Enzo, E., Giulitti, S., Cordenonsi, M., Zanconato, F., Le Digabel, J., Forcato, M., Bicciato, S. et al. (2011). Role of YAP/TAZ in mechanotransduction. *Nature* **474**, 179-183.

Eyckmans, J. and Luyten, F. P. (2006). Species specificity of ectopic bone formation using periosteum-derived mesenchymal progenitor cells. *Tissue Eng.* **12**, 2203-2213.

Eyckmans, J., Roberts, S. J., Schrooten, J. and Luyten, F. P. (2010). A clinically relevant model of osteoinduction: a process requiring calcium phosphate and BMP/Wnt signalling. *J. Cell. Mol. Med.* **14**, 1845-1856.

Eyckmans, J., Boudou, T., Yu, X. and Chen, C. S. (2011). A hitchhiker's guide to mechanobiology. *Dev. Cell* **21**, 35-47.

Gao, L., McBeath, R. and Chen, C. S. (2010). Stem cell shape regulates a chondrogenic versus myogenic fate through Rac1 and N-cadherin. *Stem Cells* **28**, 564-572.

Gomez, E. W., Chen, Q. K., Gjorevski, N. and Nelson, C. M. (2010). Tissue geometry patterns epithelial-mesenchymal transition via intercellular mechanotransduction. *J. Cell. Biochem.* **110**, 44-51.

Gómez-Barrena, E., Rosset, P., Müller, I., Giordano, R., Bunu, C., Layrolle, P., Konttinen, Y. T. and Luyten, F. P. (2011). Bone regeneration: stem cell therapies and clinical studies in orthopaedics and traumatology. *J. Cell. Mol. Med.* **15**, 1266-1286.

Hsu, S. H., Huang, G. S., Lin, S. Y., Feng, F., Ho, T. T. and Liao, Y. C. (2012). Enhanced chondrogenic differentiation potential of human gingival fibroblasts by spheroid formation on chitosan membranes. *Tissue Eng. Part A* **18**, 67-79.

Jaiswal, N., Haynesworth, S. E., Caplan, A. I. and Bruder, S. P. (1997). Osteogenic differentiation of purified, culture-expanded human mesenchymal stem cells *in vitro*. *J. Cell. Biochem.* **64**, 295-312.

Johnstone, B., Hering, T. M., Caplan, A. I., Goldberg, V. M. and Yoo, J. U. (1998). *In vitro* chondrogenesis of bone marrow-derived mesenchymal progenitor cells. *Exp. Cell Res.* **238**, 265-272.

Kilian, K. A., Bugarija, B., Lahn, B. T. and Mrksich, M. (2010). Geometric cues for directing the differentiation of mesenchymal stem cells. *Proc. Natl. Acad. Sci. USA* **107**, 4872-4877.

Kuo, J. C., Han, X., Hsiao, C. T., Yates, J. R., 3rd and Waterman, C. M. (2011). Analysis of the myosin-II-responsive focal adhesion proteome reveals a role for β-Pix in negative regulation of focal adhesion maturation. *Nat. Cell Biol.* **13**, 383-393.

Lee, H. H., Chien, C. L., Liao, H. K., Chen, Y. J. and Chang, Z. F. (2004). Nuclear efflux of heterogeneous nuclear ribonucleoprotein C1/C2 in apoptotic cells: a novel nuclear export dependent on Rho-associated kinase activation. *J. Cell Sci.* **117**, 5579-5589.

Lu, H., Guo, L., Wozniak, M. J., Kawazoe, N., Tateishi, T., Zhang, X. and Chen, G. (2009). Effect of cell density on adipogenic differentiation of mesenchymal stem cells. *Biochem. Biophys. Res. Commun.* **381**, 322-327.

Lu, Z., Doulabi, B. Z., Huang, C., Bank, R. A. and Helder, M. N. (2010). Collagen type II enhances chondrogenesis in adipose tissue-derived stem cells by affecting cell shape. *Tissue Eng. Part A* **16**, 81-90.

Maes, C., Kobayashi, T., Selig, M. K., Torrekens, S., Roth, S. I., Mackem, S., Carmeliet, G. and Kronenberg, H. M. (2010). Osteoblast precursors, but not mature osteoblasts, move into developing and fractured bones along with invading blood vessels. *Dev. Cell* **19**, 329-344.

Mahajan, A. (2012). Periosteum: a highly underrated tool in dentistry. *Int. J. Dent.* **2012**, 717816.

Mammoto, T. and Ingber, D. E. (2010). Mechanical control of tissue and organ development. *Development* **137**, 1407-1420.

Mankani, M. H., Kuznetsov, S. A. and Robey, P. G. (2007). Formation of hematopoietic territories and bone by transplanted human bone marrow stromal cells requires a critical cell density. *Exp. Hematol.* **35**, 995-1004.

Marcacci, M., Kon, E., Moukhachev, V., Lavroukov, A., Kutepov, S., Quarto, R., Mastrogiacomo, M. and Cancedda, R. (2007). Stem cells associated with macroporous bioceramics for long bone repair: 6- to 7-year outcome of a pilot clinical study. *Tissue Eng.* **13**, 947-955.

McBeath, R., Pirone, D. M., Nelson, C. M., Bhadriraju, K. and Chen, C. S. (2004). Cell shape, cytoskeletal tension, and RhoA regulate stem cell lineage commitment. *Dev. Cell* **6**, 483-495.

Miyamoto, S., Teramoto, H., Coso, O. A., Gutkind, J. S., Burbelo, P. D., Akiyama, S. K. and Yamada, K. M. (1995). Integrin function: molecular hierarchies of cytoskeletal and signaling molecules. *J. Cell Biol.* **131**, 791-805.

Nakahara, H., Dennis, J. E., Bruder, S. P., Haynesworth, S. E., Lennon, D. P. and Caplan, A. I. (1991a). *In vitro* differentiation of bone and hypertrophic cartilage from periosteal-derived cells. *Exp. Cell Res.* **195**, 492-503.

Nakahara, H., Goldberg, V. M. and Caplan, A. I. (1991b). Culture-expanded human periosteal-derived cells exhibit osteochondral potential *in vivo*. *J. Orthop. Res.* **9**, 465-476.

Nelson, C. M. and Chen, C. S. (2002). Cell-cell signaling by direct contact increases cell proliferation via a PI3K-dependent signal. *FEBS Lett.* **514**, 238-242.

Noël, D., Caton, D., Roche, S., Bony, C., Lehmann, S., Casteilla, L., Jorgensen, C. and Cousin, B. (2008). Cell specific differences between human adipose-derived and mesenchymal-stromal cells despite similar differentiation potentials. *Exp. Cell Res.* **314**, 1575-1584.

Oleynikov, Y. and Singer, R. H. (2003). Real-time visualization of ZBP1 association with beta-actin mRNA during transcription and localization. *Curr. Biol.* **13**, 199-207.

Otto, F., Thornell, A. P., Crompton, T., Denzel, A., Gilmour, K. C., Rosewell, I. R., Stamp, G. W., Beddington, R. S., Mundlos, S., Olsen, B. R. et al. (1997). Cbfa1, a candidate gene for cleidocranial dysplasia syndrome, is essential for osteoblast differentiation and bone development. *Cell* **89**, 765-771.

Pallante, B. A., Duignan, I., Okin, D., Chin, A., Bressan, M. C., Mikawa, T. and Edelberg, J. M. (2007). Bone marrow Oct3/4+ cells differentiate into cardiac myocytes via age-dependent paracrine mechanisms. *Circ. Res.* **100**, e1-e11.

Pittenger, M. F., Mackay, A. M., Beck, S. C., Jaiswal, R. K., Douglas, R., Mosca, J. D., Moorman, M. A., Simonetti, D. W., Craig, S. and Marshak, D. R. (1999). Multilineage potential of adult human mesenchymal stem cells. *Science* **284**, 143-147.

Ridley, A. J. and Hall, A. (1992). The small GTP-binding protein rho regulates the assembly of focal adhesions and actin stress fibers in response to growth factors. *Cell* **70**, 389-399.

Riveline, D., Zamir, E., Balaban, N. Q., Schwarz, U. S., Ishizaki, T., Narumiya, S., Kam, Z., Geiger, B. and Bershadsky, A. D. (2001). Focal contacts as mechanosensors: externally applied local mechanical force induces growth of focal contacts by an mDia1-dependent and ROCK-independent mechanism. *J. Cell Biol.* **153**, 1175-1186.

Sakaguchi, Y., Sekiya, I., Yagishita, K. and Muneta, T. (2005). Comparison of human stem cells derived from various mesenchymal tissues: superiority of synovium as a cell source. *Arthritis Rheum.* **52**, 2521-2529.

Schiller, H. B., Friedel, C. C., Boulegue, C. and Fässler, R. (2011). Quantitative proteomics of the integrin adhesome show a myosin II-dependent recruitment of LIM domain proteins. *EMBO Rep.* **12**, 259-266.

Seghatoleslami, M. R. and Tuan, R. S. (2002). Cell density dependent regulation of AP-1 activity is important for chondrogenic differentiation of C3H10T1/2 mesenchymal cells. *J. Cell. Biochem.* **84**, 237-248.

Sekiya, I., Larson, B. L., Vuoristo, J. T., Cui, J. G. and Prockop, D. J. (2004). Adipogenic differentiation of human adult stem cells from bone marrow stroma (MSCs). *J. Bone Miner. Res.* **19**, 256-264.

Tan, J. L., Tien, J. and Chen, C. S. (2002). Microcontact printing of proteins on mixed self-assembled monolayers. *Langmuir* **18**, 519-523.

Tan, J. L., Tien, J., Pirone, D. M., Gray, D. S., Bhadriraju, K. and Chen, C. S. (2003). Cells lying on a bed of microneedles: an approach to isolate mechanical force. *Proc. Natl. Acad. Sci. USA* **100**, 1484-1489.

Trautvetter, W., Kaps, C., Schmelzeisen, R., Sauerbier, S. and Sittinger, M. (2011). Tissue-engineered polymer-based periosteal bone grafts for maxillary sinus augmentation: five-year clinical results. *J. Oral Maxillofac. Surg.* **69**, 2753-2762.

Trounson, A., Thakar, R. G., Lomax, G. and Gibbons, D. (2011). Clinical trials for stem cell therapies. *BMC Med.* **9**, 52.

Tyndall, A. and Gratwohl, A. (2009). Adult stem cell transplantation in autoimmune disease. *Curr. Opin. Hematol.* **16**, 285-291.

Vartiainen, M. K., Guettler, S., Larijani, B. and Treisman, R. (2007). Nuclear actin regulates dynamic subcellular localization and activity of the SRF cofactor MAL. *Science* **316**, 1749-1752.

Wang, Y. K., Yu, X., Cohen, D. M., Wozniak, M. A., Yang, M. T., Gao, L., Eyckmans, J. and Chen, C. S. (2011). Bone morphogenetic protein-2-induced signaling and osteogenesis is regulated by cell shape, RhoA/ROCK, and cytoskeletal tension. *Stem Cells Dev.* **21**, 1176-1186.

Xu, Y., Wagner, D. R., Bekerman, E., Chiou, M., James, A. W., Carter, D. and Longaker, M. T. (2010). Connective tissue growth factor in regulation of RhoA mediated cytoskeletal tension associated osteogenesis of mouse adipose-derived stromal cells. *PLoS ONE* **5**, e11279.

Zhu, S. J., Choi, B. H., Huh, J. Y., Jung, J. H., Kim, B. Y. and Lee, S. H. (2006). A comparative qualitative histological analysis of tissue-engineered bone using bone marrow mesenchymal stem cells, alveolar bone cells, and periosteal cells. *Oral Surg. Oral Med. Oral Pathol. Oral Radiol. Endod.* **101**, 164-169.